

Incremental False Negative Detection for Contrastive Learning

Tsai-Shien Chen¹ Wei-Chih Hung³ Hung-Yu Tseng²
Shao-Yi Chien¹ Ming-Hsuan Yang^{2,4}

¹National Taiwan University ²University of California, Merced
³Waymo LLC ⁴Google Research

tschen@media.ee.ntu.edu.tw

Abstract

Self-supervised learning has recently shown great potential in vision tasks via contrastive learning, which aims to discriminate each image, or instance, in the dataset. However, such instance-level learning ignores the semantic relationship between instances and repels the anchor equally from the semantically similar samples, termed as “false negatives”. In this work, we first empirically highlight that the unfavorable effect from false negatives is more significant for the datasets containing images with more semantic concepts. To address the issue, we introduce a novel incremental false negative detection for self-supervised contrastive learning. Following the training process, when the encoder is gradually better-trained and the embedding space becomes more semantically structural, our method incrementally detects more reliable false negatives. Subsequently, during contrastive learning, we discuss two strategies to explicitly remove the detected false negatives. Extensive experiments show that our proposed method outperforms other self-supervised contrastive learning frameworks on multiple benchmarks within a limited compute. The source code is available at <https://github.com/tsaishien-chen/IFND>.

1 Introduction

Self-supervised learning of visual representation [12, 38, 49, 35, 30, 37, 16, 5] aims to learn a semantic-aware embedding space based on the image data without the supervision of human-labeled annotations. Recently, significant advances have been made by contrastive learning approaches [22, 41, 6, 7, 20, 8] to reduce the performance gap with supervised counterparts. Most unsupervised contrastive learning methods are developed based on the instance discrimination assumption. These approaches treat each training sample (i.e., instance) individually and learn the representations that discriminate every single sample. During training, considering an arbitrary image as an anchor, the positive samples are generated by applying different data augmentations to the anchor image, while all other images are treated as negative samples. The training objective is to maximize the distance between the anchor and the negative samples while minimizing the distances to the positives.

While instance-level contrastive learning has shown impressive performance, these methods do not take the semantic relationship between images into consideration. Despite some images share similar semantic concepts with the anchor, they are considered as negative samples and are equally pushed away from the anchor with all other negatives during training. We define these samples as “false negatives” in self-supervised contrastive learning, which would adversely affect the representation learning [39]. One might argue that such effects are minor for large-scale datasets containing images with diverse semantic concepts since the probabilities of drawing false negatives are relatively low.

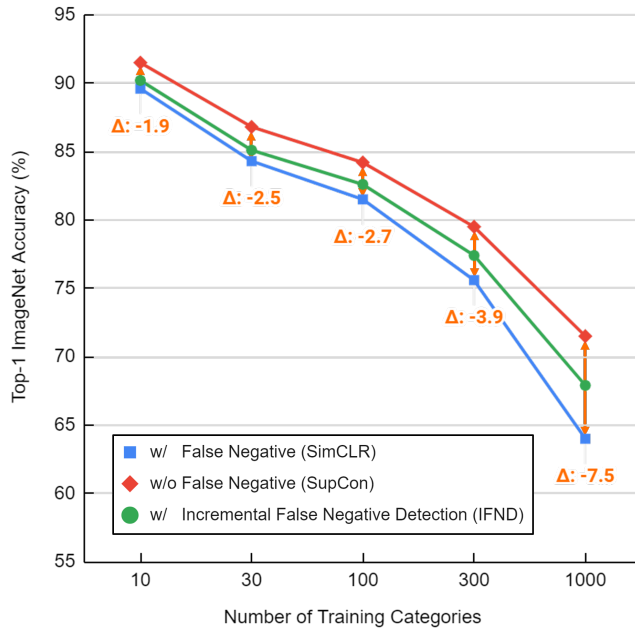


Figure 1: **Effect of false negative for contrastive learning.** To study the effect of false negatives, we compare two frameworks: SimCLR [6] (blue) representing instance-level contrastive learning trained with false negatives, and SupCon [26] (red) benefiting from human-labeled annotations to exclude false negatives. We observe that training with false negatives leads to larger performance gaps (orange) on the datasets containing images with diverse semantic concepts. The proposed approach (green) alleviates the adverse effect of false negatives for self-supervised contrastive learning. See Section 4.3 for the experiment details.

However, as shown in Figure 1, we empirically find that the undesirable effect of false negatives is more prominent on the dataset consisting of images with more diverse semantic concepts.

To handle the false negative issue, we propose to *incrementally* detect and remove *false negatives* for self-supervised contrastive learning. In the training process, we cluster samples in the intermediate learned embedding representations and assign the cluster indices as the pseudo labels to the training images. Instances with an identical label to the anchor are then detected as false negatives. However, the pseudo labels generated in the earlier training stages are not as reliable as the ones generated in the later stages since the semantic structures of the embedding space in the early stages are under development. Therefore, different from previous approaches that leverage all pseudo labels in early training stages [2, 31], we propose a novel strategy to assign the pseudo labels in an incremental manner. The key idea is to leverage the pseudo labels that are assigned with sufficient confidence. Specifically, we only use a small portion of pseudo labels with higher confidence in early training stages to detect and remove false negatives. Through the training process, we gradually include more confident labels as the encoder is better trained and the clustering algorithm can produce pseudo labels with higher quality. In addition, we discuss two loss functions to address the detected false negatives in contrastive learning, i.e., elimination and attraction, and show that the elimination is better suited for the proposed method (both theoretically and empirically). The main contributions of this paper are summarized as follows:

- We highlight the adverse effect of false negatives in contrastive learning, especially on the large-scale datasets composed of images with diverse semantic contents.
- We propose a novel contrastive learning framework with incremental false negative detection. Our approach detects and removes false negatives in an incremental manner as the embedding space becomes more semantically structural through the training process.
- Our approach performs favorably against the existing self-supervised contrastive learning frameworks on several benchmarks within the limited training resource.

2 Related Work

Instance-level contrastive learning. Learning semantic-aware visual representation without human supervision is an essential but challenging task. Numerous approaches are developed based on the instance discrimination task [13, 44, 47, 33], where each instance in the dataset is treated as an individual sample and a representation is learned to classify or contrastively separate samples. Recently, with the contrastive loss [18] and a set of image transformations or augmentations [6],

the instance-level contrastive learning methods [22, 41, 6, 7, 20, 8] achieve state-of-the-art results and even outperform some supervised pre-training approaches. While significant improvement is achieved, instance-level contrastive learning approaches typically do not take high-level semantics into account. For example, any two samples in the dataset would be considered as a negative pair and pushed apart by the contrastive loss although some of them are semantically close and should be nearby in the embedding space. When the huge amounts of negative samples (8192 for [6], 65536 for [20]) play a critical role in the success of instance-level contrastive learning, these instance-level approaches inevitably draw some “false negatives” and learn less effective representation models as shown by a recent study [39]. In this paper, we show that the performance gap between the contrastive learning trained with and without false negatives is significant on the datasets with more semantic classes (see Figure 1), and propose a progressive method to address this issue.

Semantic-aware contrastive learning. To address the limitation of instance-level contrastive learning approaches, several methods have been developed to exploit the semantic relationships between images. Chuang *et al.* [9] show that the original instance-level sampling strategy includes sampling bias and propose a debiased contrastive loss. However, this method does not explicitly detect or handle false negative samples. Huynh *et al.* [23] determine false negatives of an anchor by finding top k similar samples without referring to global embedding distribution. Khosla *et al.* [26] propose supervised contrastive losses which utilize label information and treat images of the same class as positives. Nonetheless, the annotated labels cannot be acquired in the unsupervised setting. Closely related to our method, PCL [31] discovers the representative prototypes for each semantic concept and encourages the embedding to be closer to its belonging prototype. However, there are two critical differences between PCL and the proposed method: a) during training, the loss applied in PCL does not avoid the images within the same prototype (or false negatives) being pushed apart, b) PCL uses the assigned prototype for all image regardless to the inferior clustering result in early training stages. More comparisons and discussions can be found in Section 4.4.

Clustering for deep unsupervised learning. A few unsupervised learning methods have recently leveraged clustering techniques to construct more effective representation models [2, 46, 45, 3, 51, 1]. The main idea is to use cluster indices as the pseudo label and then learn visual representation in a supervised manner. However, existing methods mainly adopt all pseudo labels to optimize the supervised loss, e.g. cross-entropy. In this work, we show that the pseudo labels obtained in earlier training processes are relatively unreliable, and the full adoption of pseudo labels in the early stage would further disrupt the representation learning. To handle this issue, we incorporate instance-level learning with clustering which allows us to only use a set of pseudo labels with sufficient confidence while treating the others as individual instances.

3 Proposed Method

3.1 Instance-Level Contrastive Learning

An instance-level contrastive learning method learns a representation that discriminates one sample from every other. Given M randomly sampled images from a training set \mathcal{X} , a contrastive training mini-batch \mathcal{I} consists of $2M$ images obtained by applying two sets of image augmentation on each sampled image. For any anchor image $i \in \mathcal{I}$, the only positive sample is another view (or transformation) of the same image, denoted as i' , while the other $2(M - 1)$ images jointly constitute the set of negative samples $\mathcal{N}(i)$. The instance-level discrimination is then optimized by the following contrastive loss:

$$\mathcal{L}_{inst} = \sum_{i \in \mathcal{I}} -\log \frac{\text{sim}(\mathbf{z}_i, \mathbf{z}_{i'})}{\sum_{s \in \mathcal{S}(i)} \text{sim}(\mathbf{z}_i, \mathbf{z}_s)}, \quad \mathcal{S}(i) \equiv \{i', n \mid n \in \mathcal{N}(i)\}, \quad (1)$$

where $\mathbf{z}_i = g(f(i))$ is the normalized embedding of image i from an encoder f and a projection head g , $\text{sim}(\mathbf{u}, \mathbf{v}) = \exp(\frac{1}{\tau} \frac{\mathbf{u} \cdot \mathbf{v}}{\|\mathbf{u}\| \|\mathbf{v}\|})$ is the similarity of two input vectors, and τ represents a temperature hyper-parameter. For instance-level contrastive learning, the negative sample set $\mathcal{N}(i)$ inevitably includes some samples with similar semantic content as the anchor i , which we term as false negatives, especially when a larger M is commonly used. Consequently, it would separate semantically similar image pairs, which is suboptimal for learning good semantic-aware visual representations.

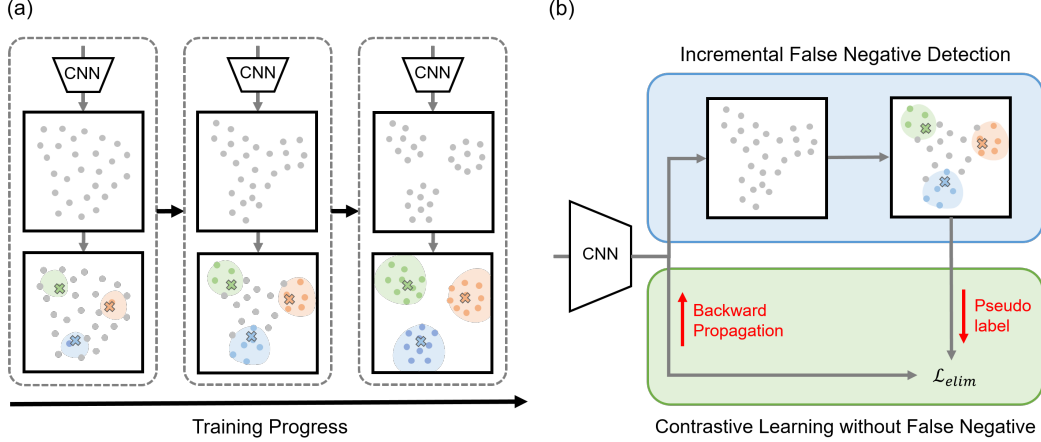


Figure 2: **Algorithmic overview.** (a) Our method uses pseudo labels in an incremental manner based on the consideration of the gradually better-trained encoder and embedding space. (b) The proposed contrastive learning framework uses pseudo labels to explicitly detect and eliminate false negatives from self-supervised contrastive learning.

3.2 Incremental False Negative Detection

To learn an effective semantic-aware embedding with self-supervised contrastive learning, our method explicitly detects the false negative samples based on the clustering results in the embedding space. Specifically, we perform k -means clustering on the features $f(i)$ of all training images $\{i \in \mathcal{X}\}$. We cluster the features into k groups and use the centroids to represent the embeddings of discovered semantic concepts. Let the centroid representation of k -th cluster be denoted as c_k . The pseudo label y_i of the image i is assigned based on the closest centroid, formally $y_i = \arg \min_k \|f(i) - c_k\|$. In the learning process, two images with identical assigned pseudo labels would be treated as a false negative pair. Nonetheless, we find that the full adoption of pseudo labels in early training processes, as in DeepCluster [2] and PCL [31], results in an undesirable learned embedding space. As illustrated in the leftmost of Figure 2(a) (or Figure 3 for a realistic case), we observe that the semantic structure of early learned embedding space is less reliable and could generate noisy pseudo labels. We quantitatively analyze this effect in Section 4.4. To tackle this problem, we incorporate instance-level learning with clustering where we only adopt the pseudo labels with higher confidence while treating the other images as individual samples. For an arbitrary image i , the desired confidence κ_i should be larger when the image embedding $f(i)$ is not only closer to the centroid of the belonging group, i.e., c_{y_i} , but also farther to the other centroids. We measure the confidence of assigned pseudo label by:

$$\kappa_i = \frac{\text{sim}(z_i, c_{y_i})}{\sum_{j=1}^k \text{sim}(z_i, c_j)}, \quad (2)$$

which is the softmax of cosine similarities between the representation of image and every centroid. We then only assign a specific rate (termed as acceptance rate) of pseudo labels with the larger confidence. As plotted in the rest part of Figure 2 (or Figure 3), with the training progressing, the encoder is better trained, and the semantic structure of embedding space is more clear which can generate more reliable pseudo labels. As a result, we propose to incrementally increase the acceptance rate. Specifically, we increase the acceptance rate linearly from 0% to 100% throughout the whole training process and empirically demonstrate that this simple strategy can achieve significant improvement in Section 4.4.

Hierarchical semantic definition. In the unsupervised setting, the precise class number of a dataset is usually unknown, and also, a different number of classes can be selected by choosing a different level of granularity. Hence, to enhance the flexibility and robustness of our method, we incorporate the hierarchical clustering techniques [25, 10, 34] to our approach. In practice, we perform multiple times of k -means with different cluster numbers to define the false negatives in the different levels of granularity. As such, the objective function (will be introduced in Section 3.3) is revised as the average of the original ones computed by the false negatives defined in different levels of granularity.

3.3 Contrastive Learning without False Negative

Given the assigned pseudo labels and detected false negatives, our goal is to revise the objective function of instance-level contrastive learning, i.e. \mathcal{L}_{inst} , to explicitly deal with the detected false negatives. Motivated by Huynh *et al.* [23], we discuss two strategies to exploit false negatives. First, the *false negative elimination* method excludes the false negative samples from the negative sample set $\mathcal{N}(i)$ for the anchor image i :

$$\mathcal{L}_{elim} = \sum_{i \in \mathcal{I}} -\log \frac{\text{sim}(\mathbf{z}_i, \mathbf{z}_{i'})}{\sum_{s \in \mathcal{S}(i)} \text{sim}(\mathbf{z}_i, \mathbf{z}_s)}, \quad \mathcal{S}(i) \equiv \{i', n \mid n \in \mathcal{N}(i), y_n \neq y_i\}. \quad (3)$$

Instead of eliminating the false negatives, the second *false negative attraction* approach considers the false negatives as the additional positive samples:

$$\mathcal{L}_{attr} = \sum_{i \in \mathcal{I}} \frac{1}{|\mathcal{P}(i)|} \sum_{p \in \mathcal{P}(i)} -\log \frac{\text{sim}(\mathbf{z}_i, \mathbf{z}_p)}{\sum_{s \in \mathcal{S}(i)} \text{sim}(\mathbf{z}_i, \mathbf{z}_s)}, \quad \begin{cases} \mathcal{S}(i) \equiv \{i', n \mid n \in \mathcal{N}(i)\} \\ \mathcal{P}(i) \equiv \{i', n \mid n \in \mathcal{N}(i), y_n = y_i\}. \end{cases} \quad (4)$$

Although SupCon [26] demonstrates the effectiveness of \mathcal{L}_{attr} with manually annotated labels, nonetheless, we theoretically show the attraction scheme applies a more aggressive strategy than the elimination approach based on their gradients (the derivation and more detailed discussions are presented in Appendix A). It results to a less tolerance to the noisy pseudo labels for \mathcal{L}_{attr} . Empirically, we also find that the elimination strategy is more stable and suitable to our method as shown in Section 4.4. Finally, we illustrate the proposed framework in Figure 2(b) and also provide the pseudo-code in Appendix B.

4 Experiments

In this section, we validate and analyze the proposed incremental false negative detection (IFND) for self-supervised contrastive learning on several benchmarks. Due to the limited training resource, we train our model on 8 Nvidia V100 GPUs for all experiments. For fair comparisons, we group prior self-supervised approaches with similar experiment setting to demonstrate the efficacy of our framework.

4.1 Implementation Details

We use ResNet-50 [21] as the encoder, following by a 3-layer MLP as the projection head to obtain 128-dimensional normalized features \mathbf{z} . We apply the proposed method on three datasets: ImageNet [11], CIFAR-10, and CIFAR-100 [28]. For the ImageNet pre-training, we follow the same setting as previous work [20, 8, 31] for fair comparisons. Specifically, we train the encoder for 200 epochs with a mini-batch size of 256 and use the memory-based method [20] to increase the number of samples for contrastive learning by maintaining a queue of instance features. For CIFAR-10 and CIFAR-100 pre-training, we train the encoder for 1000 epochs with a mini-batch size of 1024. We set the temperature parameter τ to 0.4 for all experiments. For pseudo label assignment, we use the k -means clustering implemented by Johnson *et al.* [24] to re-assign the pseudo labels after every training epoch for ImageNet, and every 20 training epochs for CIFAR (due to more training epochs and fewer training images). We use three cluster numbers to hierarchically define semantic concepts in three coarse to fine granularities for each dataset, specifically $\{10, 20, 50\}$ for CIFAR-10, $\{100, 200, 500\}$ for CIFAR-100, and $\{1000, 2000, 5000\}$ for ImageNet. We linearly increase the pseudo label acceptance rate from 0% to 100% through the whole training process and use the elimination loss \mathcal{L}_{elim} as the training objective function. More details are provided in Appendix C.

4.2 Comparison with the State-of-the-Arts

Linear evaluation and transfer learning on image classification benchmarks. We assess the performance of the image representations after pre-training on the ImageNet training set. We first train a linear classifier with the fixed representations as input on ImageNet labeled training data for linear evaluation. Furthermore, to validate the transfer capabilities, we train the linear classifier on the other two benchmarks: VOC2007 [14] and Places205 [50]. We report the Top-1 accuracy of all three datasets in Table 1. IFND obtains consistent improvements in both linear evaluation and transfer learning compared to previous self-supervised learning approaches with a similar experiment setting.

Table 1: **Linear evaluation and transfer learning on three benchmarks.** We evaluate the image representations learned with different approaches in terms of effectiveness on ImageNet [11] as well as the generality on VOC2007 [14] and Places205 [50]. We use the Top-1 classification accuracy as the metric. The upper group uses a more compact backbone (AlexNet [29] or ResNet-50 [21]) and smaller pre-training batchsize (≤ 256).

Method	Architecture	Pre-training		Datasets		
		batchsize	epochs	ImageNet	VOC2007	Places205
Jigsaw [35]	AlexNet	256	-	34.6	67.6	-
Rotation [16]	AlexNet	128	100	38.7	73.0	35.1
DeepCluster [2]	AlexNet	256	500	41.0	73.7	39.8
InstDisc [44]	ResNet-50	256	200	54.0	-	45.5
LocalAgg [51]	ResNet-50	128	200	60.2	-	50.1
SimCLR [6]	ResNet-50	256	200	64.3	-	-
CMC [41]	ResNet-50	-	200	66.2	-	-
MoCo [20]	ResNet-50	256	200	60.6	79.2	48.9
MoCo v2 [8]	ResNet-50	256	200	67.5	84.0	50.1
PCL [31]	ResNet-50	256	200	<u>67.6</u>	<u>85.4</u>	<u>50.3</u>
IFND (Ours)	ResNet-50	256	200	67.9	85.5	51.0
CPC [37]	ResNet-101	512	-	48.7	-	-
SeLa [1]	ResNet-50	1024	400	61.5	-	-
PIRL [33]	ResNet-50	1024	800	63.6	81.8	49.8
SimCLR [6]	ResNet-50	4096	1000	69.3	-	-
BYOL [17]	ResNet-50	4096	1000	74.3	-	-
SwAV [4]	ResNet-50	4096	800	75.3	88.9	56.7

Table 2: **Semi-supervised learning on ImageNet.** We report the Top-5 classification accuracy. All models are pre-trained on the whole ImageNet training set without category labels, then finetuned on 1% or 10% of ImageNet training set using the label information. The results of MoCo and MoCo v2 are computed from the officially released pre-trained models.

Method	Architecture	Pre-training		Label fraction	
		batchsize	epochs	1%	10%
InstDisc [44]	ResNet-50	256	120	39.2	77.4
MoCo [20]	ResNet-50	256	200	56.9	83.0
MoCo v2 [8]	ResNet-50	256	200	66.3	84.4
PCL [31]	ResNet-50	256	200	<u>75.3</u>	<u>85.6</u>
IFND (Ours)	ResNet-50	256	200	75.5	86.0
S4L(MOAM) [48]	ResNet-50 (4 \times)	256	1000	-	91.2
PIRL [33]	ResNet-50	1024	800	57.2	83.8
SimCLR [6]	ResNet-50	4096	1000	75.5	87.8
BYOL [17]	ResNet-50	4096	1000	78.4	89.0
SwAV [4]	ResNet-50	4096	800	78.5	89.9

Semi-supervised learning on ImageNet. Next, we evaluate the embeddings pre-training on ImageNet in the semi-supervised setting. We follow the protocol described in SimCLR [6] and use the same 1% or 10% fraction of ImageNet labeled training set to finetune the pre-trained encoder. Table 2 shows the Top-5 accuracy of the networks finetuned on two different subsets. IFND outperforms the prior approaches within the similar setup and, notably, when using 1% label, it can achieve similar performance with SimCLR trained with 16 times larger batch size and 5 times more training epochs.

4.3 Effect of False Negative Samples

In this section, we study the effect of false negatives on self-supervised contrastive learning by comparing three representative frameworks, including SimCLR [6] as instance-level learning, Sup-

Table 3: **Effect of false negatives on self-supervised learning.** We report the Top-1 classification accuracy. We use the results of SupCon, which uses the ground-truth class annotations, as the oracle performance with no effect of false negative. Δ represents the performance difference due to false negatives, and \dagger indicates that the results are quoted from the original papers. Note that we use same training epochs and batchsize for all three frameworks for fair comparison.

Method	Class label	Datasets						
		CIFAR10	CIFAR100	IN10*	IN30*	IN100*	IN300*	ImageNet
SimCLR [6]	✗	93.8 [†]	70.6	89.6	84.3	81.5	75.6	64.0 [†]
IFND (Ours)	✗	94.3	72.8	90.2	85.1	82.6	77.4	67.9
SupCon [26]	✓	96.0 [†]	76.5 [†]	91.5	86.8	84.2	79.5	71.5
Number of categories		10	100	10	30	100	300	1000
$\Delta(\text{SupCon}, \text{SimCLR})$		-2.2	-5.9	-1.9	-2.5	-2.7	-3.9	-7.5
$\Delta(\text{SupCon}, \text{IFND})$		-1.7	-3.7	-1.3	-1.7	-1.6	-2.1	-3.6

Con [26] as supervised learning using label information to exclude the false negatives and our method. We assess three frameworks on the datasets with different numbers of object categories. Note that the probability of sampling the false negatives during contrastive learning is inversely proportional to the number of classes in the dataset. We conduct the experiments on CIFAR [28] and ImageNet [11] datasets. Specifically, CIFAR-10 and CIFAR-100 have 10 and 100 classes respectively, and we sample 10, 30, 100, 300 classes from the original ImageNet (marked * in Table 3). We use the same procedure in SupCon [26] to train and conduct the linear evaluation on each dataset and show the results in Table 3.

Based on the performance drop of SimCLR compared to SupCon ($\Delta(\text{SupCon}, \text{SimCLR})$ in Table 3), we observe that the adverse effect of false negatives is more significant on the datasets with more object categories, although it is less likely to sample false negatives. Similar results are observed on both CIFAR and ImageNet. It shows that addressing the issue of sampling false negatives with instance-level contrastive learning is more important with datasets of higher diversity. With the explicit elimination of detected false negatives, we show that the proposed method can benefit self-supervised contrastive learning and reduce the performance gap from the supervised frameworks.

4.4 Strategy for False Negative Detection and Removal

In this section, we present the quantitative study on different strategies for the adoption of pseudo labels and two different schemes, i.e., elimination and attraction, to remove the detected false negatives from self-supervised contrastive learning.

Evaluation metric for measuring the clustering quality. Before presenting the quantitative analysis, we introduce the evaluation metric that measures the quality of clustering assignment first and will report it later. The pseudo labels are essentially used to detect false negatives; therefore, we compute the true positive rate [15] for each image, describing “the probability that an actual false negative (i.e., an actual positive) will be detected as a false negative sample” based on the ground truth class label. Mean true positive rate (MTPR) is then defined as the average of true positive rates of all images in the training set. On the other hand, we use mean true negative rate (MTNR) to indicate the average rate that an actual negative is still treated as a negative sample. For the existing instance-level contrastive learning methods, e.g., SimCLR [6], MTPR is 0% and MTNR is 100% since these approaches do not perform false negative detection. The goal of the proposed approach is to increase MTPR while keeping MTNR as high as possible.

Different strategies for pseudo label assignment and false negative removal. We present the quantitative comparisons between different strategies for assigning the pseudo labels and tackling the detected false negatives. The results are shown in Table 4. We conduct the experiments on CIFAR-100 and compute the MTPR nad MTNR scores on the clustering results of 100 clusters.

First, we compare three different schemes to determine the pseudo label acceptance rate, including [b] constant (DeepCluster [2]), [c] step (PCL [31]) and [g] linear (*Ours*). Our linear strategy achieves

Table 4: **Different strategies for pseudo label assignment and false negative removal.** We report MTPR (\uparrow), MTNR (\uparrow), and Top-1 accuracy on CIFAR-100. Note that, [a] is actually the instance-level learning, i.e., SimCLR [6]; [b] and [c] respectively apply the pseudo label assignment strategy used in DeepCluster [2] and PCL [31] (Step mode adopts 0% and 100% pseudo labels before and after 100 epoch over 1000 total training epochs); [g] is the final setting of the proposed method. Our linear incremental strategy produces the pseudo labels that better represent the semantic content of the images. Along with the elimination loss function, the proposed approach improves the Top-1 accuracy from 70.6 to 72.8 on CIFAR-100, compared to the instance-level contrastive learning.

Index	Acceptance Rate of Pseudo Label			Objective	MTPR	MTNR	Top-1 Acc.
	Scheme	Initial	Final				
[a]	Constant	0%	0%	\mathcal{L}_{inst}	0	100	70.6
[b]	Constant	100%	100%	\mathcal{L}_{elim}	29.80	99.05	69.6
[c]	Step	0%	100%	\mathcal{L}_{elim}	<u>37.69</u>	99.36	71.3
[d]	Linear	0%	25%	\mathcal{L}_{elim}	12.61	99.97	70.9
[e]	Linear	0%	50%	\mathcal{L}_{elim}	23.36	99.87	71.9
[f]	Linear	0%	75%	\mathcal{L}_{elim}	33.25	99.74	<u>72.5</u>
[g]	Linear	0%	100%	\mathcal{L}_{elim}	41.12	99.56	72.8
[h]	Linear	0%	100%	\mathcal{L}_{attr}	26.59	98.82	68.4

both higher MTPR and MTNR compared to the constant and step strategy. The results validate that the proposed linear incremental strategy effectively finds the false negatives, and then, improves the performance of self-supervised contrastive learning.

We then analyze the effect of using different final acceptance rates ([d,e,f,g]) for the linear strategy. Intuitively, higher acceptance rates for assigning the pseudo labels indicate more false negatives are detected (MTPR increases) but more true negatives are also improperly found and removed (MTNR decreases). However, we find that using the 100% final acceptance rate ([g]) improves MTPR to 41.12% with only a slight MTNR dropping of 0.44% compared to the instance-level contrastive learning approach (i.e., 0% final acceptance rate). Along with the elimination loss described in Eq. 3, we improve the downstream Top-1 classification accuracy from 70.6% to 72.8%

Finally, we compare the elimination and attraction loss functions described in Section 3.3 ([g,h]). With different strategies to address the detected false negatives, we find that the learned embeddings through minimizing \mathcal{L}_{attr} are unstable and more rely on the good quality of pseudo labels. Notably, this observation is consistent to the theoretical analysis in Appendix A indicating that compared to \mathcal{L}_{elim} , \mathcal{L}_{attr} applies a more aggressive scheme which would pull the instance embeddings with same given pseudo labels closer and therefore, would be more sensitive to the quality of the pseudo label. Empirically, the model supervised by \mathcal{L}_{attr} performs even worse than the instance-level learning.

4.5 Visualization of Embedding Space

In Figure 3, we visualize the learned embedding spaces and corresponding pseudo label assignments in different training stages using t-SNE [42]. We use the CIFAR-10 dataset for clear visualization. As shown in the leftmost part of Figure 3, the semantic structure of the embedding space in 100 epoch is still under-developed and, therefore, the generated pseudo labels are not reliable to represent the semantic relationship among instances. Taking the issue into account, IFND only adopts a little portion of pseudo labels with higher confidence scores in early stages. Later in training processes, with the better-trained encoder and more semantically structural embedding space, incrementally including more pseudo labels can benefit the semantic-aware representation learning.

Subsequently, we compare the learned embedding spaces among SimCLR [6], SupCon [26], and our approach in Figure 4. It shows that the embedding space trained by our method has more compact clusters than the one learned from instance-level learning. Compared to SimCLR, IFND can produce a more structural embedding space which is also more similar to the one trained by the supervised framework (SupCon). More visualizations and discussions can be found in Appendix D.

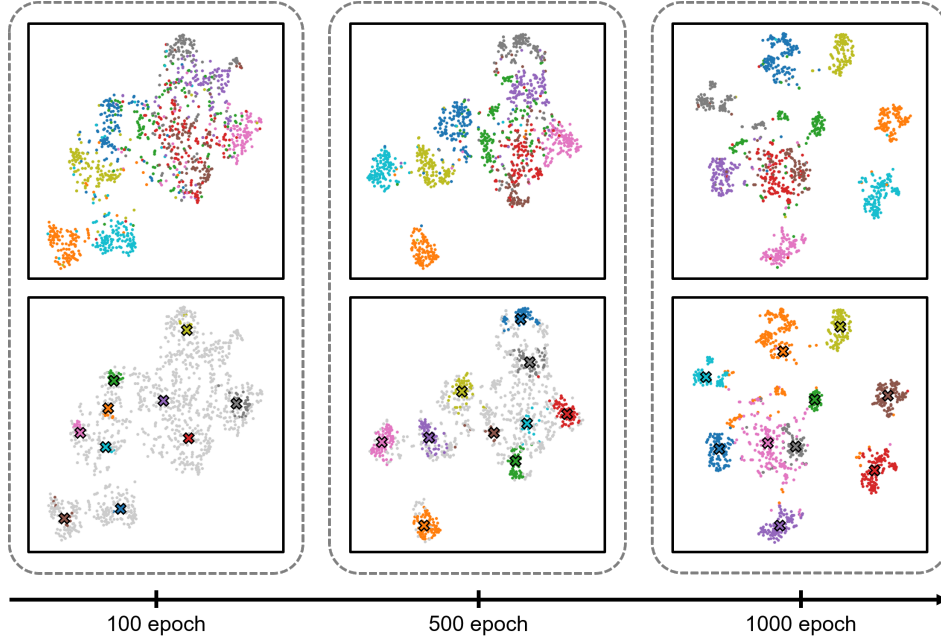


Figure 3: **Visualization of embedding spaces and pseudo label assignments in different training stages on CIFAR-10.** The samples in the upper/lower row are colored with the ground true label/assigned pseudo label respectively. \times marks are the cluster centroids and light grey dots represent the instances without assigned pseudo labels. IFND accepts the pseudo label in an incremental manner considering that the learned embedding spaces gradually become more semantically structural and can progressively generate more reliable pseudo labels.

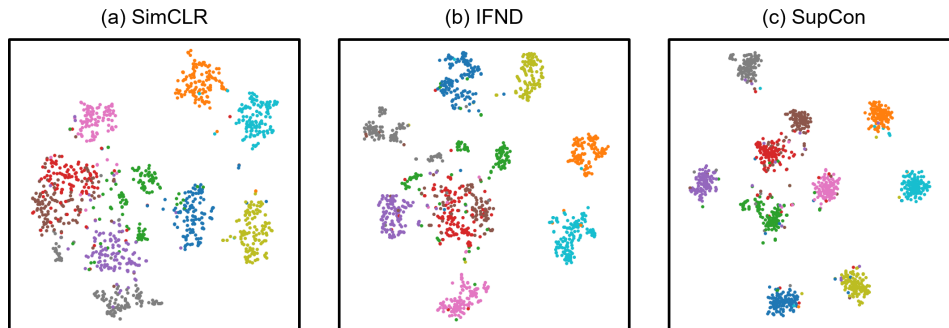


Figure 4: **Visualization of learned embedding spaces by different methods on CIFAR-10.** Compared to instance-level contrastive learning, i.e. SimCLR [6], our framework can learn the embedding space with a more clear semantic structure and is more similar to the learned representations trained by the supervised framework, i.e. SupCon [26].

5 Conclusion

In this work, we empirically analyze the undesired impact of false negatives for self-supervised contrastive learning. To mitigate such adverse effects, we then introduce an incremental false negative detection approach to progressively detect and remove the false negatives through the training stage. Extensive experiment results validate the effectiveness of the proposed framework on several benchmarks and also demonstrate the capability to reduce the gap from the supervised framework.

References

- [1] Yuki Markus Asano, Christian Rupprecht, and Andrea Vedaldi. Self-labelling via simultaneous clustering and representation learning. In *International Conference on Learning Representations*, 2020. 3, 6
- [2] Mathilde Caron, Piotr Bojanowski, Armand Joulin, and Matthijs Douze. Deep clustering for unsupervised learning of visual features. In *European Conference on Computer Vision*, 2018. 2, 3, 4, 6, 7, 8
- [3] Mathilde Caron, Piotr Bojanowski, Julien Mairal, and Armand Joulin. Unsupervised pre-training of image features on non-curated data. In *IEEE International Conference on Computer Vision*, 2019. 3
- [4] Mathilde Caron, Ishan Misra, Julien Mairal, Priya Goyal, Piotr Bojanowski, and Armand Joulin. Unsupervised learning of visual features by contrasting cluster assignments. In *Advances in Neural Information Processing Systems*, 2020. 6
- [5] Mark Chen, Alec Radford, Rewon Child, Jeffrey Wu, Heewoo Jun, David Luan, and Ilya Sutskever. Generative pretraining from pixels. In *International Conference on Machine Learning*, 2020. 1
- [6] Ting Chen, Simon Kornblith, Mohammad Norouzi, and Geoffrey Hinton. A simple framework for contrastive learning of visual representations. In *International Conference on Machine Learning*, 2020. 1, 2, 3, 6, 7, 8, 9, 15
- [7] Ting Chen, Simon Kornblith, Kevin Swersky, Mohammad Norouzi, and Geoffrey E Hinton. Big self-supervised models are strong semi-supervised learners. In *Advances in Neural Information Processing Systems*, 2020. 1, 3
- [8] Xinlei Chen, Haoqi Fan, Ross Girshick, and Kaiming He. Improved baselines with momentum contrastive learning. *arXiv preprint arXiv:2003.04297*, 2020. 1, 3, 5, 6, 15
- [9] Ching-Yao Chuang, Joshua Robinson, Yen-Chen Lin, Antonio Torralba, and Stefanie Jegelka. Debaised contrastive learning. In *Advances in Neural Information Processing Systems*, 2020. 3
- [10] Florence Corpet. Multiple sequence alignment with hierarchical clustering. *Nucleic acids research*, pages 10881–10890, 1988. 4
- [11] Jia Deng, Wei Dong, Richard Socher, Li-Jia Li, Kai Li, and Li Fei-Fei. Imagenet: A large-scale hierarchical image database. In *IEEE Conference on Computer Vision and Pattern Recognition*, 2009. 5, 6, 7, 15
- [12] Carl Doersch, Abhinav Gupta, and Alexei A Efros. Unsupervised visual representation learning by context prediction. In *IEEE International Conference on Computer Vision*, 2015. 1
- [13] Alexey Dosovitskiy, Philipp Fischer, Jost Tobias Springenberg, Martin Riedmiller, and Thomas Brox. Discriminative unsupervised feature learning with exemplar convolutional neural networks. *IEEE Transactions on Pattern Analysis and Machine Intelligence*, pages 1734–1747, 2015. 2
- [14] Mark Everingham, Luc Van Gool, Christopher KI Williams, John Winn, and Andrew Zisserman. The pascal visual object classes (voc) challenge. *International Journal of Computer Vision*, pages 303–338, 2010. 5, 6
- [15] Tom Fawcett. An introduction to roc analysis. *Pattern Recognition Letters*, 2006. 7
- [16] Spyros Gidaris, Praveer Singh, and Nikos Komodakis. Unsupervised representation learning by predicting image rotations. In *International Conference on Learning Representations*, 2018. 1, 6
- [17] Jean-Bastien Grill, Florian Strub, Florent Altché, Corentin Tallec, Pierre Richemond, Elena Buchatskaya, Carl Doersch, Bernardo Avila Pires, Zhaohan Guo, Mohammad Gheshlaghi Azar, Bilal Piot, koray kavukcuoglu, Remi Munos, and Michal Valko. Bootstrap your own latent: A new approach to self-supervised learning. In *Advances in Neural Information Processing Systems*, 2020. 6
- [18] Michael Gutmann and Aapo Hyvärinen. Noise-contrastive estimation: A new estimation principle for unnormalized statistical models. In *International Conference on Artificial Intelligence and Statistics*, 2010. 2
- [19] Ben Harwood, Vijay Kumar BG, Gustavo Carneiro, Ian Reid, and Tom Drummond. Smart mining for deep metric learning. In *IEEE International Conference on Computer Vision*, 2017. 13, 14
- [20] Kaiming He, Haoqi Fan, Yuxin Wu, Saining Xie, and Ross Girshick. Momentum contrast for unsupervised visual representation learning. In *IEEE Conference on Computer Vision and Pattern Recognition*, 2020. 1, 3, 5, 6, 15
- [21] Kaiming He, Xiangyu Zhang, Shaoqing Ren, and Jian Sun. Deep residual learning for image recognition. In *IEEE Conference on Computer Vision and Pattern Recognition*, 2016. 5, 6, 15

- [22] R Devon Hjelm, Alex Fedorov, Samuel Lavoie-Marchildon, Karan Grewal, Phil Bachman, Adam Trischler, and Yoshua Bengio. Learning deep representations by mutual information estimation and maximization. In *International Conference on Learning Representations*, 2019. 1, 3
- [23] Tri Huynh, Simon Kornblith, Matthew R Walter, Michael Maire, and Maryam Khademi. Boosting contrastive self-supervised learning with false negative cancellation. *arXiv preprint arXiv:2011.11765*, 2020. 3, 5
- [24] Jeff Johnson, Matthijs Douze, and Hervé Jégou. Billion-scale similarity search with gpus. *IEEE Transactions on Big Data*, 2019. 5
- [25] Stephen C Johnson. Hierarchical clustering schemes. *Psychometrika*, pages 241–254, 1967. 4
- [26] Prannay Khosla, Piotr Teterwak, Chen Wang, Aaron Sarna, Yonglong Tian, Phillip Isola, Aaron Maschinot, Ce Liu, and Dilip Krishnan. Supervised contrastive learning. In *Advances in Neural Information Processing Systems*, 2020. 2, 3, 5, 7, 8, 9, 14, 15
- [27] Jack Kiefer, Jacob Wolfowitz, et al. Stochastic estimation of the maximum of a regression function. *The Annals of Mathematical Statistics*, 1952. 15
- [28] Alex Krizhevsky, Geoffrey Hinton, et al. Learning multiple layers of features from tiny images. 2009. 5, 7, 15
- [29] Alex Krizhevsky, Ilya Sutskever, and Geoffrey E Hinton. Imagenet classification with deep convolutional neural networks. In *Advances in Neural Information Processing Systems*, 2012. 6
- [30] Gustav Larsson, Michael Maire, and Gregory Shakhnarovich. Colorization as a proxy task for visual understanding. In *IEEE Conference on Computer Vision and Pattern Recognition*, 2017. 1
- [31] Junnan Li, Pan Zhou, Caiming Xiong, and Steven Hoi. Prototypical contrastive learning of unsupervised representations. In *International Conference on Learning Representations*, 2021. 2, 3, 4, 5, 6, 7, 8, 15
- [32] Ilya Loshchilov and Frank Hutter. Sgdr: Stochastic gradient descent with warm restarts. *arXiv preprint arXiv:1608.03983*, 2016. 15
- [33] Ishan Misra and Laurens van der Maaten. Self-supervised learning of pretext-invariant representations. In *IEEE Conference on Computer Vision and Pattern Recognition*, 2020. 2, 6
- [34] Fionn Murtagh and Pierre Legendre. Ward’s hierarchical agglomerative clustering method: which algorithms implement ward’s criterion? *Journal of classification*, pages 274–295, 2014. 4
- [35] Mehdi Noroozi and Paolo Favaro. Unsupervised learning of visual representations by solving jigsaw puzzles. In *European Conference on Computer Vision*, 2016. 1, 6
- [36] Hyun Oh Song, Yu Xiang, Stefanie Jegelka, and Silvio Savarese. Deep metric learning via lifted structured feature embedding. In *IEEE Conference on Computer Vision and Pattern Recognition*, 2016. 13, 14
- [37] Aaron van den Oord, Yazhe Li, and Oriol Vinyals. Representation learning with contrastive predictive coding. *arXiv preprint arXiv:1807.03748*, 2018. 1, 6
- [38] Deepak Pathak, Philipp Krahenbuhl, Jeff Donahue, Trevor Darrell, and Alexei A Efros. Context encoders: Feature learning by inpainting. In *IEEE Conference on Computer Vision and Pattern Recognition*, 2016. 1
- [39] Nikunj Saunshi, Orestis Plevrakis, Sanjeev Arora, Mikhail Khodak, and Hrishikesh Khandeparkar. A theoretical analysis of contrastive unsupervised representation learning. In *International Conference on Machine Learning*, 2019. 1, 3
- [40] Florian Schroff, Dmitry Kalenichenko, and James Philbin. Facenet: A unified embedding for face recognition and clustering. In *IEEE Conference on Computer Vision and Pattern Recognition*, 2015. 14
- [41] Yonglong Tian, Dilip Krishnan, and Phillip Isola. Contrastive multiview coding. *arXiv preprint arXiv:1906.05849*, 2019. 1, 3, 6
- [42] Laurens Van der Maaten and Geoffrey Hinton. Visualizing data using t-sne. *Journal of machine learning research*, 2008. 8
- [43] Chao-Yuan Wu, R Manmatha, Alexander J Smola, and Philipp Krahenbuhl. Sampling matters in deep embedding learning. In *IEEE International Conference on Computer Vision*, 2017. 13, 14
- [44] Zhirong Wu, Yuanjun Xiong, Stella X Yu, and Dahua Lin. Unsupervised feature learning via non-parametric instance discrimination. In *IEEE Conference on Computer Vision and Pattern Recognition*, 2018. 2, 6
- [45] Junyuan Xie, Ross Girshick, and Ali Farhadi. Unsupervised deep embedding for clustering analysis. In *International Conference on Machine Learning*, 2016. 3

- [46] Jianwei Yang, Devi Parikh, and Dhruv Batra. Joint unsupervised learning of deep representations and image clusters. In *IEEE Conference on Computer Vision and Pattern Recognition*, 2016. [3](#)
- [47] Mang Ye, Xu Zhang, Pong C Yuen, and Shih-Fu Chang. Unsupervised embedding learning via invariant and spreading instance feature. In *IEEE Conference on Computer Vision and Pattern Recognition*, 2019. [2](#)
- [48] Xiaohua Zhai, Avital Oliver, Alexander Kolesnikov, and Lucas Beyer. S4l: Self-supervised semi-supervised learning. In *IEEE International Conference on Computer Vision*, 2019. [6](#)
- [49] Richard Zhang, Phillip Isola, and Alexei A Efros. Split-brain autoencoders: Unsupervised learning by cross-channel prediction. In *IEEE Conference on Computer Vision and Pattern Recognition*, 2017. [1](#)
- [50] Bolei Zhou, Agata Lapedriza, Jianxiong Xiao, Antonio Torralba, and Aude Oliva. Learning deep features for scene recognition using places database. In *Advances in Neural Information Processing Systems*, 2014. [5](#), [6](#)
- [51] Chengxu Zhuang, Alex Lin Zhai, and Daniel Yamins. Local aggregation for unsupervised learning of visual embeddings. In *IEEE International Conference on Computer Vision*, 2019. [3](#), [6](#)

A Theoretical Analysis for Elimination and Attraction Losses

In Section 3.3, we claim that the attraction loss \mathcal{L}_{attr} (Eq. 4) uses a more aggressive strategy than the elimination loss \mathcal{L}_{elim} (Eq. 3) to handle the detected false negatives. In this section, we provide the theoretical justification by analyzing the gradient produced by these two loss functions. Furthermore, we demonstrate that they have the inherent capability of hard sample mining [36, 19, 43]. Without loss of generality, we use i to represent an arbitrary anchor image, and re-write the two losses as:

$$\mathcal{L}_{elim,i} = -\log \frac{\exp(\mathbf{z}_i \cdot \mathbf{z}_{i'}/\tau)}{\sum_{s \in \mathcal{S}(i)} \exp(\mathbf{z}_i \cdot \mathbf{z}_s/\tau)}, \quad \mathcal{S}(i) \equiv \{i', n \mid n \in \mathcal{N}(i), y_n \neq y_i\} \quad , \text{ and} \quad (5)$$

$$\mathcal{L}_{attr,i} = \frac{1}{|\mathcal{P}(i)|} \sum_{p \in \mathcal{P}(i)} -\log \frac{\exp(\mathbf{z}_i \cdot \mathbf{z}_p/\tau)}{\sum_{s \in \mathcal{S}(i)} \exp(\mathbf{z}_i \cdot \mathbf{z}_s/\tau)}, \quad \begin{cases} \mathcal{S}(i) \equiv \{i', n \mid n \in \mathcal{N}(i)\} \\ \mathcal{P}(i) \equiv \{i', n \mid n \in \mathcal{N}(i), y_n = y_i\}. \end{cases} \quad (6)$$

We then derive the gradient of $\mathcal{L}_{elim,i}$ in Eq. 5 with regard to the embedding of anchor image, i.e. \mathbf{z}_i :

$$\begin{aligned} \frac{\partial \mathcal{L}_{elim,i}}{\partial \mathbf{z}_i} &= \frac{\partial}{\partial \mathbf{z}_i} -\log \frac{\exp(\mathbf{z}_i \cdot \mathbf{z}_{i'}/\tau)}{\sum_{s \in \mathcal{S}(i)} \exp(\mathbf{z}_i \cdot \mathbf{z}_s/\tau)} \\ &= \frac{\partial}{\partial \mathbf{z}_i} \log \sum_{s \in \mathcal{S}(i)} \exp(\mathbf{z}_i \cdot \mathbf{z}_s/\tau) - \frac{\partial}{\partial \mathbf{z}_i} \log(\exp(\mathbf{z}_i \cdot \mathbf{z}_{i'}/\tau)) \\ &= \sum_{s \in \mathcal{S}(i)} \left(\frac{\exp(\mathbf{z}_i \cdot \mathbf{z}_s/\tau)}{\sum_{s \in \mathcal{S}(i)} \exp(\mathbf{z}_i \cdot \mathbf{z}_s/\tau)} \cdot \frac{\mathbf{z}_s}{\tau} \right) - \frac{\mathbf{z}_{i'}}{\tau} \\ &= \sum_{\substack{n \in \mathcal{N}(i), \\ y_n \neq y_i}} \left(\frac{\exp(\mathbf{z}_i \cdot \mathbf{z}_n/\tau)}{\sum_{s \in \mathcal{S}(i)} \exp(\mathbf{z}_i \cdot \mathbf{z}_s/\tau)} \cdot \frac{\mathbf{z}_n}{\tau} \right) - \left(1 - \frac{\exp(\mathbf{z}_i \cdot \mathbf{z}_{i'}/\tau)}{\sum_{s \in \mathcal{S}(i)} \exp(\mathbf{z}_i \cdot \mathbf{z}_s/\tau)} \right) \cdot \frac{\mathbf{z}_{i'}}{\tau} \\ &= \sum_{\substack{n \in \mathcal{N}(i), \\ y_n \neq y_i}} \frac{\sigma_n^-}{\tau} \mathbf{z}_n - \frac{\sigma_{i'}^+}{\tau} \mathbf{z}_{i'}, \end{aligned} \quad (7)$$

where

$$\begin{aligned} \sigma_x^- &= \frac{\exp(\mathbf{z}_i \cdot \mathbf{z}_x/\tau)}{\sum_{s \in \mathcal{S}(i)} \exp(\mathbf{z}_i \cdot \mathbf{z}_s/\tau)} = \frac{\text{sim}(\mathbf{z}_i, \mathbf{z}_x)}{\sum_{s \in \mathcal{S}(i)} \text{sim}(\mathbf{z}_i \cdot \mathbf{z}_s)} \quad , \text{ and} \\ \sigma_x^+ &= 1 - \frac{\exp(\mathbf{z}_i \cdot \mathbf{z}_x/\tau)}{\sum_{s \in \mathcal{S}(i)} \exp(\mathbf{z}_i \cdot \mathbf{z}_s/\tau)} = 1 - \frac{\text{sim}(\mathbf{z}_i, \mathbf{z}_x)}{\sum_{s \in \mathcal{S}(i)} \text{sim}(\mathbf{z}_i \cdot \mathbf{z}_s)} \end{aligned} \quad (8)$$

are the coefficient terms respectively for the negative or positive sample x .

Next, the gradient of $\mathcal{L}_{attr,i}$ in Eq. 6 is derived in a similar way:

$$\begin{aligned}
\frac{\partial \mathcal{L}_{attr,i}}{\partial \mathbf{z}_i} &= \frac{\partial}{\partial \mathbf{z}_i} \frac{1}{|\mathcal{P}(i)|} \sum_{p \in \mathcal{P}(i)} -\log \frac{\exp(\mathbf{z}_i \cdot \mathbf{z}_p / \tau)}{\sum_{s \in \mathcal{S}(i)} \exp(\mathbf{z}_i \cdot \mathbf{z}_s / \tau)} \\
&= \frac{1}{|\mathcal{P}(i)|} \sum_{p \in \mathcal{P}(i)} \left(\frac{\partial}{\partial \mathbf{z}_i} \log \sum_{s \in \mathcal{S}(i)} \exp(\mathbf{z}_i \cdot \mathbf{z}_s / \tau) - \frac{\partial}{\partial \mathbf{z}_i} \log \exp(\mathbf{z}_i \cdot \mathbf{z}_p / \tau) \right) \\
&= \frac{1}{|\mathcal{P}(i)|} \sum_{p \in \mathcal{P}(i)} \left[\sum_{s \in \mathcal{S}(i)} \left(\frac{\exp(\mathbf{z}_i \cdot \mathbf{z}_s / \tau)}{\sum_{s \in \mathcal{S}(i)} \exp(\mathbf{z}_i \cdot \mathbf{z}_s / \tau)} \cdot \frac{\mathbf{z}_s}{\tau} \right) - \frac{\mathbf{z}_p}{\tau} \right] \\
&= \sum_{s \in \mathcal{S}(i)} \left(\frac{\exp(\mathbf{z}_i \cdot \mathbf{z}_s / \tau)}{\sum_{s \in \mathcal{S}(i)} \exp(\mathbf{z}_i \cdot \mathbf{z}_s / \tau)} \cdot \frac{\mathbf{z}_s}{\tau} \right) - \sum_{p \in \mathcal{P}(i)} \frac{1}{|\mathcal{P}(i)|} \frac{\mathbf{z}_p}{\tau} \\
&= \sum_{\substack{n \in \mathcal{N}(i), \\ y_n \neq y_i}} \left(\frac{\exp(\mathbf{z}_i \cdot \mathbf{z}_n / \tau)}{\sum_{s \in \mathcal{S}(i)} \exp(\mathbf{z}_i \cdot \mathbf{z}_s / \tau)} \cdot \frac{\mathbf{z}_n}{\tau} \right) \\
&\quad - \sum_{p \in \mathcal{P}(i)} \left(\frac{1}{|\mathcal{P}(i)|} - \frac{\exp(\mathbf{z}_i \cdot \mathbf{z}_p / \tau)}{\sum_{s \in \mathcal{S}(i)} \exp(\mathbf{z}_i \cdot \mathbf{z}_s / \tau)} \right) \cdot \frac{\mathbf{z}_p}{\tau} \\
&= \sum_{\substack{n \in \mathcal{N}(i), \\ y_n \neq y_i}} \frac{\sigma_n^-}{\tau} \mathbf{z}_n - \sum_{p \in \mathcal{P}(i)} \frac{\sigma_p^+}{\tau} \mathbf{z}_p,
\end{aligned} \tag{9}$$

where

$$\begin{aligned}
\sigma_x^- &= \frac{\exp(\mathbf{z}_i \cdot \mathbf{z}_x / \tau)}{\sum_{s \in \mathcal{S}(i)} \exp(\mathbf{z}_i \cdot \mathbf{z}_s / \tau)} = \frac{\text{sim}(\mathbf{z}_i, \mathbf{z}_x)}{\sum_{s \in \mathcal{S}(i)} \text{sim}(\mathbf{z}_i \cdot \mathbf{z}_s)} \quad , \text{ and} \\
\sigma_x^+ &= \frac{1}{|\mathcal{P}(i)|} - \frac{\exp(\mathbf{z}_i \cdot \mathbf{z}_x / \tau)}{\sum_{s \in \mathcal{S}(i)} \exp(\mathbf{z}_i \cdot \mathbf{z}_s / \tau)} = \frac{1}{|\mathcal{P}(i)|} - \frac{\text{sim}(\mathbf{z}_i, \mathbf{z}_x)}{\sum_{s \in \mathcal{S}(i)} \text{sim}(\mathbf{z}_i \cdot \mathbf{z}_s)}.
\end{aligned} \tag{10}$$

The gradients in Eq. 7 and Eq. 9 actually share a similar form to the gradient of triplet loss [40] representing the fundamental manner of \mathcal{L}_{elim} and \mathcal{L}_{attr} to attract positive sample(s) while repelling negative samples.[†] We can then find that both \mathcal{L}_{elim} and \mathcal{L}_{attr} similarly remove the detected false negatives (i.e. $\{n \mid n \in \mathcal{N}(i), y_n = y_i\}$) from the negative samples. Moreover, \mathcal{L}_{attr} considers the detected false negatives as the additional positive samples (i.e. $\mathcal{P}(i) \equiv \{i', n \mid n \in \mathcal{N}(i), y_n = y_i\}$). Therefore, \mathcal{L}_{attr} applies a more aggressive strategy which not only avoids the false negatives being push apart from the anchors but also pulls the false negatives close to the anchors.

Additionally, consistent to the finding from Khosla *et al.* [26], the coefficient terms σ_x^+ and σ_x^- in Eq. 8 and Eq. 10 are determined by $\text{sim}(\mathbf{z}_i, \mathbf{z}_x)$. Larger coefficients are given when the negative/positive samples are more similar/dissimilar to the anchor. This observation indicates that these two loss functions have the implicit capability of hard sample mining [36, 19, 43], i.e., focusing on differentiating the “hard negatives” that are near the anchors or attracting the “hard positives” which are far away from the anchors.

[†]The gradient of triplet loss $\left([\|\mathbf{z}_i - \mathbf{z}_p\|_2^2 - \|\mathbf{z}_i - \mathbf{z}_a\|_2^2 + \alpha]^+ \right)$ w.r.t \mathbf{z}_i is $(2\mathbf{z}_n - 2\mathbf{z}_p)$

B Pseudo Code

Algorithm 1: Contrastive Learning with Incremental False Negative Detection

Input : encoder f , projection head g , training samples \mathcal{X} , and number of clusters k
// instance-level contrastive learning in the beginning

```

1 Initialize completely different pseudo label  $y^*$  for each sample
2 while  $Epoch \in Training\ Epoch$  do
    // contrastive learning with false negative elimination
3   for mini-batch  $\mathcal{I}$  do
4      $z = g(f(\{i \sim \mathcal{I}\}))$ 
5     update encoder  $f$  and projection head  $g$  to minimize  $\mathcal{L}_{elim}(z, y^*)$ 
6   end
7   if  $Epoch \in Clustering\ Epoch$  then                                // pseudo label assignment
8      $v = f(\{x \sim \mathcal{X}\})$ 
9      $c, y = k\text{-means}(v, k)$ 
10     $\kappa = \text{sim}(z, c_y) / \sum_{j=1}^k \text{sim}(z, c_j)$ 
11    determine the acceptance rate of pseudo label as  $(Epoch / Training\ Epoch)$ 
12    update pseudo label  $y^*$  by a fraction of  $y$  with larger  $\kappa$ 
13  end
14 end

```

C Pre-Training and Evaluation Details

As described in Section 4.1, we use the proposed method to pre-train ResNet-50 [21] on ImageNet [11], CIFAR-10, and CIFAR-100 [28]. For ImageNet pre-training, we follow the setting of previous work [20, 8] that uses SGD optimizer [27] with a weight decay of 0.0001 and a momentum of 0.9. The learning rate is set to 0.03 initially which is then multiplied by 0.1 at 120 and 160 epochs. For CIFAR-10 and CIFAR-100 pre-training, we also use SGD optimizer with the same weight decay and momentum. But, we set the initial learning rate to 0.5 and use a linear warm-up strategy for the first 10 epochs. In the rest of the training, we decay the learning rate with the cosine annealing schedule [32].

For linear evaluation on ImageNet, we train the classifier (a fully connected layer followed by softmax) with the fixed pre-trained representations for 100 epochs. Following the the same hyper-parameter setting used in the previous work [31], we optimize the model by SGD optimizer with a batch size of 256, an initial learning rate of 10, a momentum of 0.9, and a weight decay of 0. As for the semi-supervised learning, we fine-tune the pre-trained ResNet-50 model and the classifier using the subsets of 1% or 10% ImageNet labeled training data (note that we use the same subsets of ImageNet training data as SimCLR [6]). The model is trained using SGD optimizer for 20 epochs, a batch size of 256, a momentum of 0.9, and a weight decay of 0.0005. The learning rate for ResNet-50 is 0.01 while the one for the linear classifier is 0.1 (for 10% ImageNet) or 1 (for 1% ImageNet). All learning rates are multiplied by 0.2 at 12 and 16 epochs.

D Visualization of Learned Embedding Space through Training Process

In this section, we visualize and compare the embedding spaces learned by four contrastive learning frameworks, including (a) SimCLR [6], (b) IFND (trained by \mathcal{L}_{attr}), (c) IFND (trained by \mathcal{L}_{elim}), and (d) SupCon [26], through the training process. The results are shown in Figure 5.

Compared to IFND trained by \mathcal{L}_{elim} , the one trained by \mathcal{L}_{attr} learns the embedding spaces with more concentrated clusters which are more similar to SupCon due to using same attraction objective function. However, during training, the unsupervised clustering would inevitably produce some noisy pseudo labels (as supported by the MTNR in Table 4 being less than 100%). Consequently, the attraction loss may inappropriately pull the true negative samples closer to the anchor. We can then find that although the learned embedding space in the rightmost of Figure 5(b) shows more concentrated clusters, nonetheless, a cluster is not actually constituted by the image embeddings

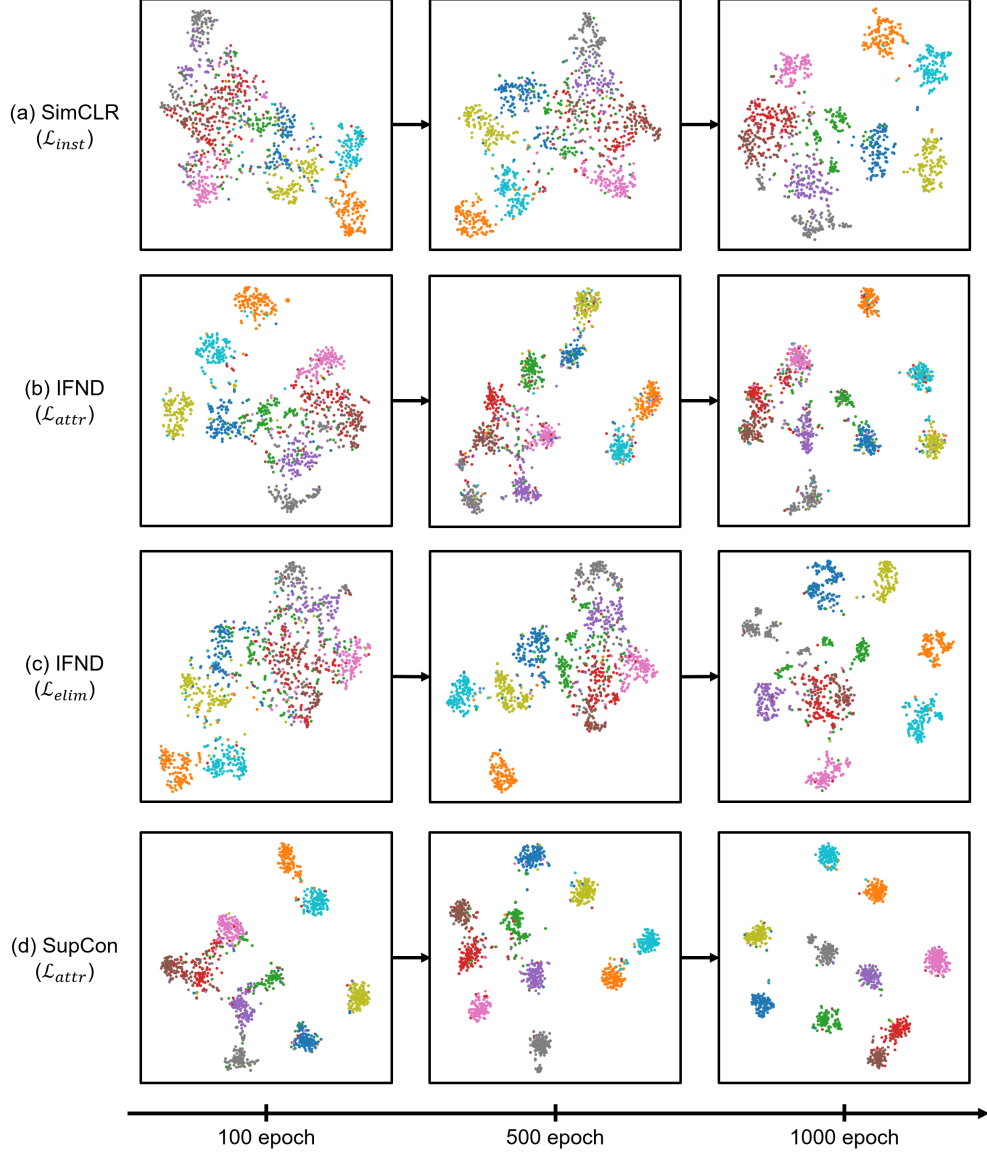


Figure 5: **Visualization of embedding spaces on CIFAR-10.** We compare four contrastive learning frameworks based on their learned embedding spaces through the training process. We list their respective objective functions in the bracket.

representing the same semantic content. Also, as shown in Table 4, the attraction loss leads to inferior representation performance compared to the elimination objective.

As for IFND trained by \mathcal{L}_{elim} , which is the final proposed method, it learns a similar embedding space as SimCLR in the early stage, since the acceptance rate for assigning the pseudo label is still low and the proposed framework behaves like the instance-level contrastive learning (e.g., SimCLR) in earlier processes. However, with more reliable pseudo labels generated in later stages, \mathcal{L}_{elim} avoids more detected false negatives being pushed apart from the anchor, and finally learns a more favorable embedding space compared to SimCLR.